Light-Induced Conformational Changes of Rhodopsin Probed by Fluorescent Alexa594 Immobilized on the Cytoplasmic Surface†

Yasushi Imamoto,*,‡ Mikio Kataoka,‡ Fumio Tokunaga,§ and Krzysztof Palczewski*,||

Graduate School of Materials Science, Nara Institute of Science and Technology, Ikoma, Nara 630-0101, Japan, Department of Earth and Space Science, Graduate School of Science, Osaka University, Toyonaka, Osaka 560-0043, Japan, and Departments of Ophthalmology, Pharmacology, and Chemistry, University of Washington, Seattle, Washington 98195

Received August 9, 2000; Revised Manuscript Received October 11, 2000

ABSTRACT: A novel fluorescence method has been developed for detecting the light-induced conformational changes of rhodopsin and for monitoring the interaction between photolyzed rhodopsin and G-protein or arrestin. Rhodopsin in native membranes was selectively modified with fluorescent Alexa594−maleimide at the Cys^{316} position, with a large excess of the reagent Cys^{140} that was also derivatized. Modification with Alexa594 allowed the monitoring of fluorescence changes at a red excitation light wavelength of 605 nm, thus avoiding significant rhodopsin bleaching. Upon absorption of a photon by rhodopsin, the fluorescence intensity increased as much as 20% at acidic pH with an apparent pK_a of ∼6.8 at 4 °C, and was sensitive to the presence of hydroxylamine. These findings indicated that the increase in fluorescence is specific for metarhodopsin II. In the presence of transducin, a significant increase in fluorescence was observed. This increase of fluorescence emission intensity was reduced by addition of GTP, in agreement with the fact that transducin enhances the formation of metarhodopsin II. Under conditions that favored the formation of a metarhodopsin II−Alexa594 complex, transducin slightly decreased the fluorescence. In the presence of arrestin, under conditions that favored the formation of metarhodopsin I or II, a phosphorylated, photolyzed rhodopsin−Alexa594 complex only slightly decreased the fluorescence intensity, suggesting that the cytoplasmic surface structure of metarhodopsin II is different in the complex with arrestin and transducin. These results demonstrate the application of Alexa594-modified rhodopsin (Alexa594−rhodopsin) to continuously monitor the conformational changes in rhodopsin during light-induced transformations and its interactions with other proteins.

Upon absorption of a photon in the vertebrate retina, the 11-*cis*-retinal chromophore of rhodopsin is isomerized to *all-trans*-retinal (*1*, *2*). This 11-*cis*-retinal chromophore forms a protonated Schiff base with a Lys^{296} residue located within the hydrophobic core of the seven-transmembrane helical segment of rhodopsin (*3*−*5*). Fast photoisomerization of the chromophore leads to formation of high-energy rhodopsin intermediates, distinguished by their characteristic absorption spectra, beginning with the formation of photorhodopsin, bathorhodopsin, lumirhodopsin, and metarhodopsin I, which relaxes to the signaling form of the receptor called metarhodopsin II. Ultimately, metarhodopsin II decays to opsin and free *all-trans*-retinal (*6*). During this bleaching process, changes occur in the protonation and hydrogen-bonding states of several rhodopsin residues (*5*, *7*−*11*) and the retinylidene Schiff base. These changes influence the absorption properties of the photolyzed rhodopsin; for example, the absorption maximum of metarhodopsin II is ∼380 nm due to the deprotonation of the Schiff base (*12*). The structure of the cytoplasmic surface of rhodopsin is altered upon formation of metarhodopsin II (*13*), and three proteins [G-protein (transducin), arrestin, and rhodopsin kinase] bind to this region of the activated receptor (*14*−*19*). The binding of transducin and arrestin is specific for metarhodopsin II (*20*−*23*) or/and phosphorylated metarhodopsin II (*24*), respectively. The primary site of the interaction for transducin, rhodopsin kinase, and arrestin is located within the loop region between helices V and VI on the cytoplasmic side of photolyzed rhodopsin (*25*−*27*). To understand the signal transduction pathways utilized by rhodopsin, and other G-protein-coupled receptors, it is important to elucidate the kinetics and binding specificity of photolyzed rhodopsin during this signaling process under conditions as close as possible to the native settings.

Because the intensity and maximal wavelength of fluorescence are sensitive to environmental changes, fluorescent dyes are excellent probes for detecting local conformational changes in proteins. However, due to the extremely high

† This work was supported in part by the Novartis Foundation, the Kansai Research Foundation for Technology Promotion, NIH Grant EY08061, an unrestricted grant from Research to Prevent Blindness, Inc. (RPB, New York, NY), to the Department of Ophthalmology at the University of Washington, a grant from the Ruth and Milton Steinbach Fund, and the E. K. Bishop Foundation.

* To whom correspondence should be addressed. Y.I.: Graduate School of Materials Science, Nara Institute of Science and Technology, Ikoma, Nara 630-0101, Japan; phone, +81-743-72-6101; fax, +81-743-72-6109; e-mail, imamoto@ms.aist-nara.ac.jp. K.P.: Department of Ophthalmology, University of Washington, Box 356485, Seattle, WA 98195-6485; phone, (206) 543-9074; fax, (206) 221-6784; e-mail, palczews@u.washington.edu.

‡ Nara Institute of Science and Technology.

§ Osaka University.

|| University of Washington.

10.1021/bi0018685 CCC: $19.00
Published on Web 11/11/2000

photosensitivity of rhodopsin at wavelengths used for common fluorophore excitation, typical procedures would cause bleaching of the pigment. To avoid this problem, a fluorophore with a longer maximal excitation wavelength (λ_{max}) is required. Recently, derivatives of Texas Red, Alexa594, and Cy5 have became available (*28*−*30*), which absorb sufficiently at wavelengths >600 nm, and therefore can be used for excitation without significant bleaching of rhodopsin.

For protein modification, the chemistries of amino and sulfhydro groups are widely employed. However, because rhodopsin has multiple Lys residues on the cytoplasmic side, the cysteine residues appear to be more useful for selective modification. Bovine rhodopsin has 10 cysteine residues at positions 110, 140, 167, 185, 187, 222, 264, 316, 322, and 323 (*4*, *31*). Among them, Cys^{110} and Cys^{187} form a disulfide bond, Cys^{322} and Cys^{323} are palmitoylated (*32*), and Cys^{167}, Cys^{222}, and Cys^{264} are buried within the transmembrane helices. On the basis of numerous studies, Cys^{140} and Cys^{316}, located at the cytoplasmic side, have been found to be reactive with respect to maleimide and iodoacetamide. From these two residues, Cys^{316} appears to be more reactive (*33*−*36*). In the study presented here, light-induced conformational changes of rhodopsin in native membranes and its interaction with G-protein or arrestin were investigated by a novel continuous fluorescence method. Cys^{316} was selectively modified with fluorescent Alexa594−maleimide, and photon absorption by rhodopsin increased the fluorescence intensity up to 20%. This method allowed us to monitor the metarhodopsin I−metarhodopsin II transition and the binding of interacting proteins, transducin and arrestin.

MATERIALS AND METHODS

Preparation of Rod Outer Segments (ROS).[1] ROS were isolated from frozen bovine retina by a conventional sucrose flotation method {40% (w/v) in ROS buffer [10 mM MOPS, 30 mM NaCl, 60 mM KCl, and 2 mM $MgCl_2$ (pH 7.5)]}, followed by a stepwise sucrose gradient method [29 to 36% (w/v)] (*37*). ROS were washed with buffer A [5 mM Tris-HCl and 0.5 mM $MgCl_2$ (pH 7.2)] supplemented with 0.3 mM EDTA, and then with buffer A. ROS membranes were collected by centrifugation at 109000*g* for 30 min.

Phosphorylation of Rhodopsin. Photolyzed rhodopsin in ROS was phosphorylated by endogenous rhodopsin kinase in the presence of 5 mM ATP (*14*). The resulting phosphorylated opsin was regenerated to rhodopsin by addition of a 2-fold molar excess of 11-*cis*-retinal followed by incubation at room temperature overnight.

Modification of Rhodopsin in ROS Membranes by Alexa594−*Maleimide.* Typically, ROS containing 3.8 mg (95 nmol) of rhodopsin were suspended in 500 μL of 50 mM sodium phosphate buffer (pH 7.0). Ten (sample 1), 20 (sample 2), or 80 μL (sample 3) of the Alexa594 solution (10 mg/mL in DMSO, Molecular Probes) (110, 220, or 880 nmol, respectively) was added to the ROS suspension, and the reaction mixture was incubated at room temperature for 15 h. The reaction was terminated with 35 μL of 55 mM glutathione and the mixture kept on ice for 30 min to inactivate maleimide. The modified membrane was washed once with 4 M urea (109000*g* for 30 min), twice with buffer A (109000*g* for 30 min), and twice with ROS buffer (27200*g* for 30 min).

Table 1: Molar Ratio of Rhodopsin to Alexa594 at the Various Stages of Purification[a]

sample no.	reaction mixture[b]	buffer wash[b]	urea wash[b]	Con A purification[b]
1	1:9.3	1:3.0	1:2.6	1:1.51
2	1:2.3	−	1:1.7	1:0.93
3	1:1.2	−	1:0.8	1:0.30

[a] The modification of rhodopsin with Alexa594 was carried out as described in Materials and Methods. [b] The ratio of rhodopsin to Alexa594.

Stoichiometry. The Alexa594−rhodopsin complex (~0.1 mg of rhodopsin in 40 μL) was dissolved by addition of 4.4 μL of a 7.5% CHAPS solution. The mixture was mixed with a suspension of concanavalin A−Sepharose (~200 μL), equilibrated with CHAPS buffer [0.75% CHAPS and 10 mM Tris-HCl (pH 7.4)], and incubated at 4 °C overnight. Concanavalin A−Sepharose was washed with CHAPS buffer. The Alexa594−rhodopsin complex was eluted from concanavalin A−Sepharose by 300 mM methyl α-D-mannopyranoside in 300 μL of CHAPS buffer. The elution procedure was repeated once. The concentration of Alexa594 was measured by absorbance at 590 nm (molar extinction coefficient of 96 000), and the rhodopsin concentration was measured by an absorbance decrease at 500 nm (molar extinction coefficient of 40 600) (*38*), after exposure to light in the presence of 50 mM hydroxylamine. The molar ratio of Alexa594 to rhodopsin for samples 1−3 (see above) was estimated to be 0.3:1, 0.9:1, and 1.5:1, respectively (Table 1).

Thermolysin Digestion of the Alexa594−*Rhodopsin Complex*. The Alexa594−rhodopsin complex (60−200 μg) (samples 1−3, respectively) was suspended in 24.5 μL of 10 mM Tris-HCl (pH 7.4) containing 5 mM $CaCl_2$ and 0.04 mg/mL thermolysin. The digestion reaction mixture was incubated at 37 °C for 80 min, and the reaction was terminated by adding 5 μL of 50 mM EDTA. The sample was kept at −80 °C until it was used, and the test for completeness of digestion and separation of fragments was carried out employing SDS−PAGE, using a 15% acrylamide gel. The fluorophore bands were first visualized by UV illumination; thereafter, protein bands were stained by Coomassie Brilliant Blue.

Preparation of Transducin and Arrestin. Transducin was prepared by a GTP extraction method (*15*). Briefly, ROS isolated by the stepwise sucrose gradient method were suspended in ROS buffer and incubated for 30 min on ice under room light. Bleached ROS were washed with buffer A supplemented with 0.3 mM EDTA, and then with buffer A. The membranes were collected by centrifugation at 109000*g* for 30 min. Finally, ROS were suspended in buffer A. Immediately after addition of GTP at a final concentration of 20 μM, the sample was centrifuged at 109000*g* for 30 min. Transducin was collected in the supernatant, and the extraction was repeated again. GTP was removed by repeat-

[1] Abbreviations: CHAPS, 3-[(3-cholamidopropyl)dimethylammonio]-propanesulfonic acid; EDTA, ethylenediaminetetraacetic acid; HEPES, *N*-(2-hydroxyethyl)piperazine-*N*′-2-ethanesulfonic acid; MES, 2-morpholinoethanesulfonic acid; MOPS, 3-(*N*-morpholino)propanesulfonic acid; ROS, rod outer segments; SDS−PAGE, sodium dodecyl sulfate−polyacrylamide gel electrophoresis.

ing the concentration with ultrafiltration (Amicon) and dilution by buffer A.

Arrestin was prepared by DEAE-cellulose (Whatman) and heparin−Sepharose (Pharmacia) column chromatography as reported previously (*39*).

Spectroscopy. Absorption and fluorescence spectra were recorded with a Hewlett-Packard model 8452A photodiode array spectrophotometer and a Perkin-Elmer model LS50B spectrofluorometer, respectively. The sample cell holder of the spectrofluorometer was equipped with a temperature controlling system and a magnetic stirrer. For the fluorescence measurements (Figures 2B−7), the intact or phosphorylated ROS membrane, which had been modified by Alexa594 in about 1:1 stoichiometry, was suspended in the buffer described in the figure legends and put in the optical cell (1 cm × 1 cm). For the binding assay, transducin or arrestin was added to the sample. The volume of the reaction mixture was 1.8 mL. The sample was continuously stirred and kept at constant temperature. Rhodopsin in ROS was photolyzed with a camera strobe flash lamp (Sunpak 433D) at the top of the sample compartment, which bleached 60% of the rhodopsin. Exposure of the sample to the excitation beam of the spectrofluorometer at 605 nm for 30 min bleached <4% of the rhodopsin.

RESULTS

Selection of the Fluorescent Probe for Modifying Rhodopsin. Fluorescent dyes with long excitation wavelengths offer the opportunity to monitor continuous interactions between rhodopsin and interacting proteins, because the excitation beam of the fluorometer would not bleach rhodopsin significantly. From this standpoint, Alexa594, Texas Red, and Cy5 appeared to be the most useful reagents with absorption maxima at 588, 582, and 649 nm, respectively. In terms of spectroscopic properties, including quantum yield, Texas Red and Cy5 appeared to be the best among them; however, fluorescence probes are often hydrophobic and therefore partition into a membrane layer, or are complex structures and may not modify rhodopsin efficiently. If the measurements were performed in a native lipid environment, multiple copies of the fluorophore bound to the membranes would cause a significant increase in the light-independent background, and lower the sensitivity of the assay. Similary, a low stoichiometry of modification would also lower the sensitivity. Experimentally, we first estimated the molar ratio of rhodopsin and these fluorophores after incubation with ROS followed by several washes with buffer. The fluorophore:rhodopsin ratio was 2 for the Alexa594−maleimide complex, 7 for the Texas Red−maleimide complex, and 0.03 for the Cy5−iodoacetoamide complex. These results suggested that Texas Red partitions largely to the membrane due to its hydrophobicity, whereas Cy5 was an inefficient modifier of rhodopsin and was washed out by the buffer. Therefore, Alexa594 was used in the experiments described below.

Stoichiometry of Rhodopsin Modification by Alexa594. The stoichiometry of rhodopsin modification with Alexa594 was tested under several conditions. Alexa594, not removed by washes from ROS membranes, may not necessarily be bound to rhodopsin, but rather may be inserted into membranes or modify proteins other than rhodopsin. The stoichiometry of rhodopsin modification by Alexa594 was determined from a molar ratio of rhodopsin and Alexa594 in the various stages of the modification and purification procedures, including washes with buffer A, 4 M urea, and after purification by concanavalin A−Sepharose (Table 1). The amount of Alexa594 was measured from the absorbance at 590 nm (molar extinction coefficient of 96 000), and the amount of rhodopsin was measured from an absorbance decrease at 500 nm (molar extinction coefficient of 40 600) (*38*) after irradiation in the presence of 50 mM hydroxylamine. The stoichiometry was determined to be between 0.3 and 1.51 (Table 1) under different conditions.

Localization of the Site of Modification. Of all the cysteins, Cys^{140} and Cys^{316} are the most reactive; both are located on the cytoplasmic surface of rhodopsin (for example, see refs *40* and *41*) (Figure 1A). To determine which of these two groups is modified with Alexa594, we took advantage of the fact that rhodopsin is cleaved by thermolysin at the loop region between helices V and VI (*40*, *42*). As a result of rhodopsin cleavage with thermolysin, a long fragment (containing reactive Cys^{140}) and a shorter fragment (containing the second reactive Cys^{316}) were generated. These two fragments are readily separated by SDS−PAGE. When modified rhodopsins with different concentrations of Alexa594 were digested with thermolysin and subjected to SDS−PAGE separation (Figure 1B), the band of uncleaved rhodopsin, long (F1) and short (F2) fragments were detected. Prior to staining, the Alexa594 bands were also visualized by UV illumination (Figure 1C). The fluorescence bands corresponding to undigested rhodopsin and the short fragment were observed in all lanes. However, the long fragment F1 containing Cys^{140} was only modified with the highest concentration of Alexa594. Therefore, F2 containing Cys^{316} was exclusively modified at low concentrations of the Alexa594 reagent, when the molar ratio of Alexa594 to rhodopsin in the reaction mixture was <2.3. The following experiments were carried out employing the Alexa594−rhodopsin complex in a 1:0.9 stoichiometry (sample 2). Although we did not formally prove the site of modification by Alexa594, the hydrophilic character of the probe would prevent its incorporation into the interior of the hydrophobic transmembrane domain of rhodopsin. In addition, Cys^{140} and Cys^{316} are only accessible for chemical modification on the cytoplasmic surface (*5*). Therefore, it is reasonable to speculate that Cys^{316} is exclusively modified at the low concentration of Alexa594.

Spectroscopic Properties of the Alexa594−Rhodopsin Complex. Typical absorption spectra of the Alexa594−rhodopsin complex solubilized in CHAPS buffer are shown in Figure 2A. The difference spectrum before and after irradiation of the Alexa594−rhodopsin complex (inset of Figure 2A) in the presence of 50 mM hydroxylamine is identical to the bleaching curve of native rhodopsin (not shown), indicating that modification with Alexa594 did not alter the spectrum of rhodopsin. The fluorescence spectra of ROS membranes with and without the fluorophore were also recorded using excitation at 605 nm (Figure 2B). The former is the sum of scattering of the excitation beam and fluorescence, whereas the latter is only scattering. As shown in panels B and C of Figure 2, the scattering of the excitation beam was negligible at wavelengths >20 nm from the

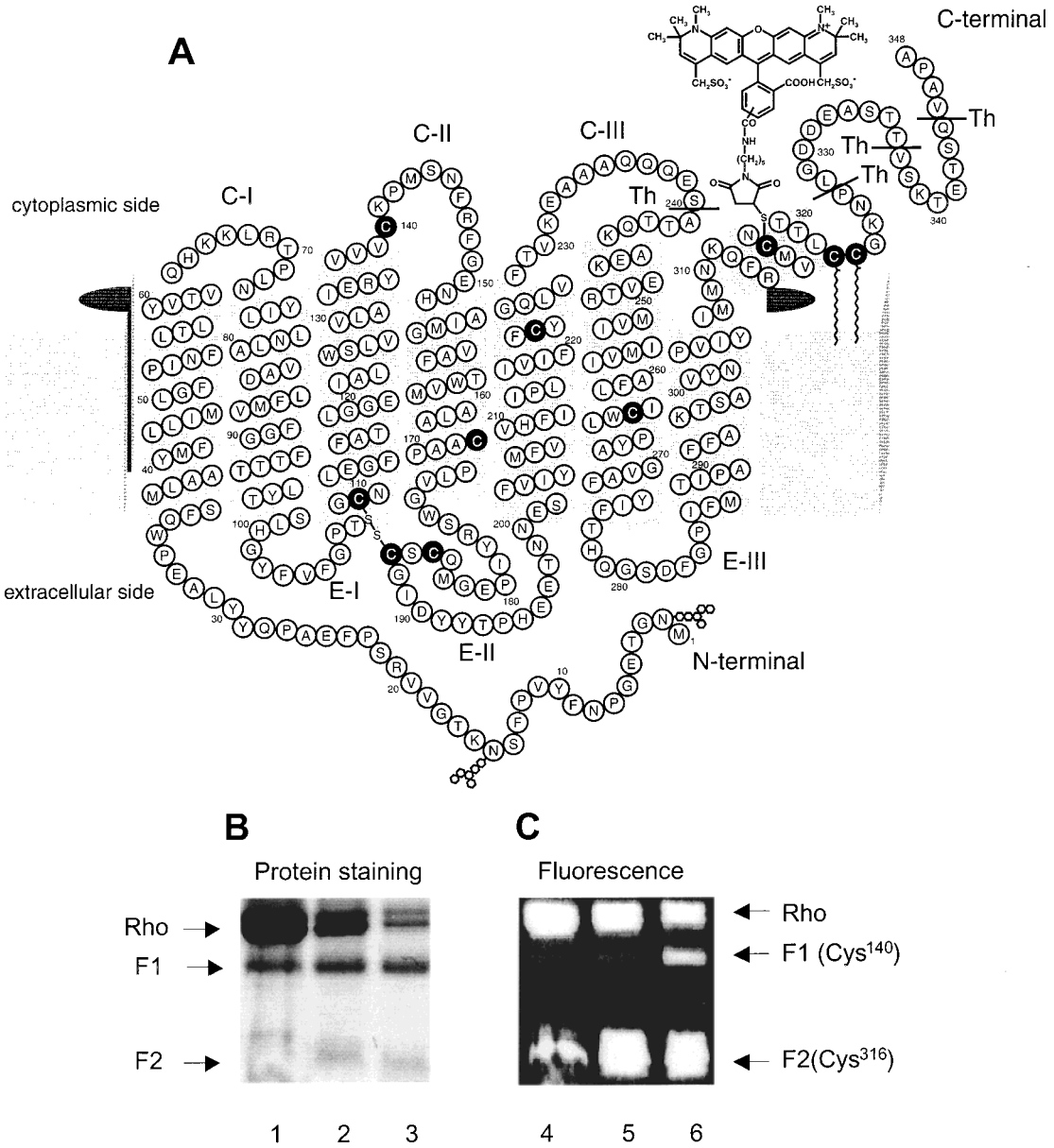

FIGURE 1: Identification of the modification site on rhodopsin by Alexa594−maleimide. Washed ROS, containing mostly rhodopsin, were modified with increasing amounts of Alexa594 (samples 1−3; see Materials and Methods). Next, rhodopsin was digested by thermolysin and subjected to SDS−PAGE (samples 1−3 are lanes 1−3, respectively). The thermolytic F1 fragment contains Cys^{140}, whereas the F2 fragment contains Cys^{316}. Note that at lower concentrations of Alexa594−maleimide, only the F2 fragment was modified. (A) Model of rhodopsin showing the most likely localization of Cys residues and cleavage sites by thermolysin (Th). Cys^{316} is the primary site of modification by Alexa594 (the structure shown in the panel). The model is based on the crystal structure of bovine rhodopsin (*5*). (B) Proteins on SDS−PAGE gel were visualized with Coomassie Brilliant Blue. Note that the amount of rhodopsin is different among samples. (C) The fluorescent bands were visualized under UV illumination. The level of incorporation of the fluorescent probe into other bands than rhodopsin fragments was less than 4% throughout remaining regions of gel. The amounts of the samples loaded per lane were chosen to contain roughly the same amount of the fluorophore.

maximum of the excitation beam. In the experiments described below, the sample was excited at 605 nm and the fluorescence was monitored at 630 nm. Exposure of the sample to the excitation beam at 605 nm for 30 min bleached <4% of the rhodopsin.

Temperature and pH Dependence of the Photolyzed Alexa594−Rhodopsin Complex. The Alexa594−rhodopsin complex was suspended in MES buffer (pH 5.9), and the fluorescence at 630 nm was monitored (Figure 3). Upon photolysis of rhodopsin, an increase in fluorescence was observed. At 4 °C, the increased fluorescence was stable for >2000 s. However, at 15 and 25 °C, the fluorescence decreased with time. In contrast, the fluorescence is further increased in the presence of hydroxylamine and there was no further decay. This increase in fluorescence upon flash is attributed to the formation of the equilibrium between metarhodopsin I and metarhodopsin II, and the decay to the formation of metarhodopsin III. This is consistent with an earlier report that the metarhodopsin I and metarhodopsin II equilibrium is temperature-sensitive (*43*−*45*). In the presence of hydroxylamine, metarhodopsins would decay to opsin, in which the fluorescence is most intense. This is an unexpected result, as it is generally assumed that the structure of rhodopsin and opsin is very similar. The Alexa594−

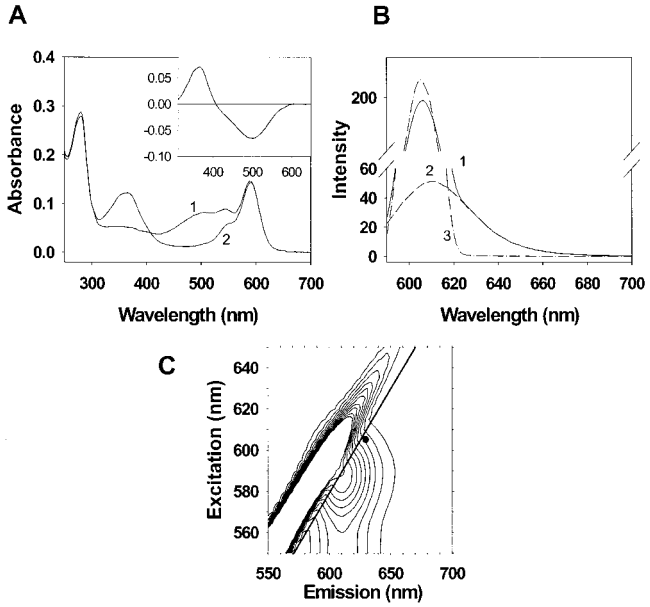

FIGURE 2: Absorption and fluorescence spectra of the Alexa594−rhodopsin conjugate. (A) The absorption spectra of the Alexa594−rhodopsin conjugate before and after the bleach of rhodopsin. The Alexa594−rhodopsin conjugate was solubilized by 0.75% CHAPS buffer in the presence of 50 mM hydroxylamine (trace 1). It was irradiated for 5 min (trace 2), and the difference spectrum between curves 1 and 2 was calculated (inset). (B) Fluorescence and scattering of the excitation beam. The emission spectrum of the Alexa594−rhodopsin conjugate (35 nM) in HEPES buffer [50 mM HEPES, 140 mM NaCl, and 2 mM $MgCl_2$ (pH 7.5)] with the excitation at 605 nm (solid line, trace 1) was composed of the fluorescence of Alexa594 (recorded with 560 nm excitation, broken line, trace 2) and scattering of excitation light at 605 nm (−•−). (C) Three-dimensional spectrum of excitation wavelength, emission wavelength, and fluorescence intensity. The fluorescence signal at 630 nm is minimally affected by the scattering of the excitation beam at 605 nm (●). Contours are drawn every 10 units of arbitrary fluorescence intensity.

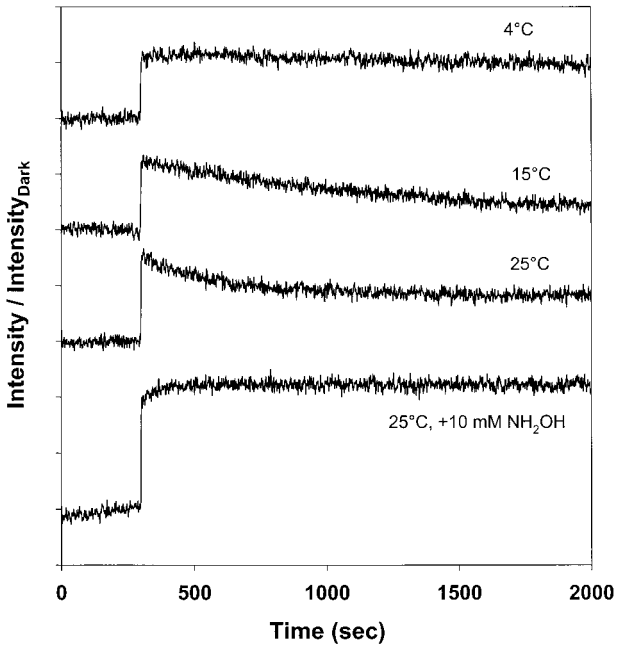

FIGURE 3: Temperature dependence of the fluorescence increase after flash excitation of rhodopsin. The Alexa594−rhodopsin conjugate (35 nM) was suspended in 50 mM MES buffer (pH 5.9) at 4, 15, and 25 °C. Rhodopsin was photoactived 300 s after recording had begun by a flash that bleached ∼60% of the rhodopsin. The last sample was supplemented with 10 mM hydroxylamine and incubated at 25 °C prior to the experiment. The excitation and emission wavelengths were set at 605 and 630 nm, respectively.

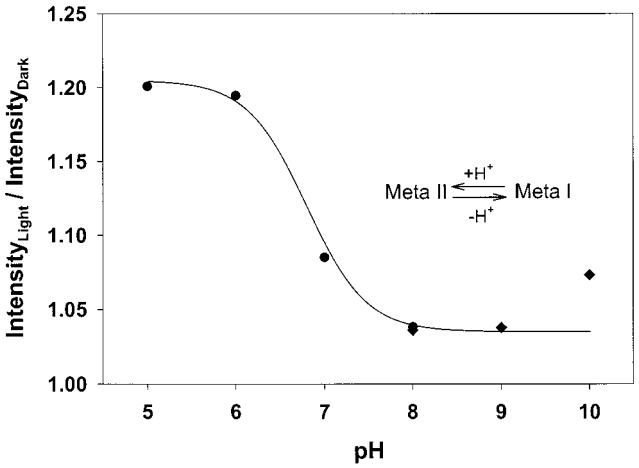

FIGURE 4: pH dependence of the fluorescence after flash excitation of rhodopsin. The Alexa594−rhodopsin conjugate (125 nM) was suspended in 20 mM phosphate buffer at pH 5−8 (●) or borate buffer at pH 8−10 (◆) containing 140 mM NaCl at 4 °C. The ratio of fluorescence intensity before and after flash excitation was plotted vs pH. The excitation and emission wavelengths were set at 605 and 630 nm, respectively.

rhodopsin complex could be a useful tool for discriminating between opsin and rhodopsin structures.

The equilibrium between metarhodopsin I and metarhodopsin II is pH-sensitive (*43*, *44*, *46*). Thus, we measured the transition between metarhodopsin I and metarhodopsin II using our fluorescence methods. The Alexa594−rhodopsin complex was suspended in phosphate buffer (pH 5−8) or borate buffer (pH 8−10), and changes in the fluorescence intensity before and after rhodopsin bleaching by flash were measured (Figure 4). The fluorescence increase at pH 5−6 was 20%, whereas the increase at pH 8−9 was 3−5%. The apparent pK_a was 6.8, which is in good agreement with the pK_a between metarhodopsin I and metarhodopsin II reported previously (*44*, *46*). Because metarhodopsin II is dominant under acidic conditions, the fluorescence increase is mainly due to the formation of metarhodopsin II. The fluorescence intensity of metarhodopsin I was 4% larger than that of rhodopsin, as shown at pH 9.0. The fluorescence increased again at pH 10, most likely due to rhodopsin denaturation (Figure 4).

Interaction between the Photolyzed Alexa594−Rhodopsin Complex and Transducin. A typical result of binding experiments between the Alexa594−rhodopsin complex and transducin is shown in Figure 5A. The Alexa594−rhodopsin complex was suspended in buffer, and the fluorescence at 630 nm with excitation at 605 nm was monitored. The rhodopsin was activated by a flash at 120 s, and the sample was supplemented with GTP at 360 s. Without transducin, the fluorescence upon the flash increased and was insensitive to addition of GTP. In the presence of transducin, however, three changes in fluorescence were observed. First, a rapid increase in fluorescence was observed soon after the flash. This change was much faster than the time resolution in our experimental setup. The second change was a slow increase in fluorescence, which took about 50 s to reach a plateau.

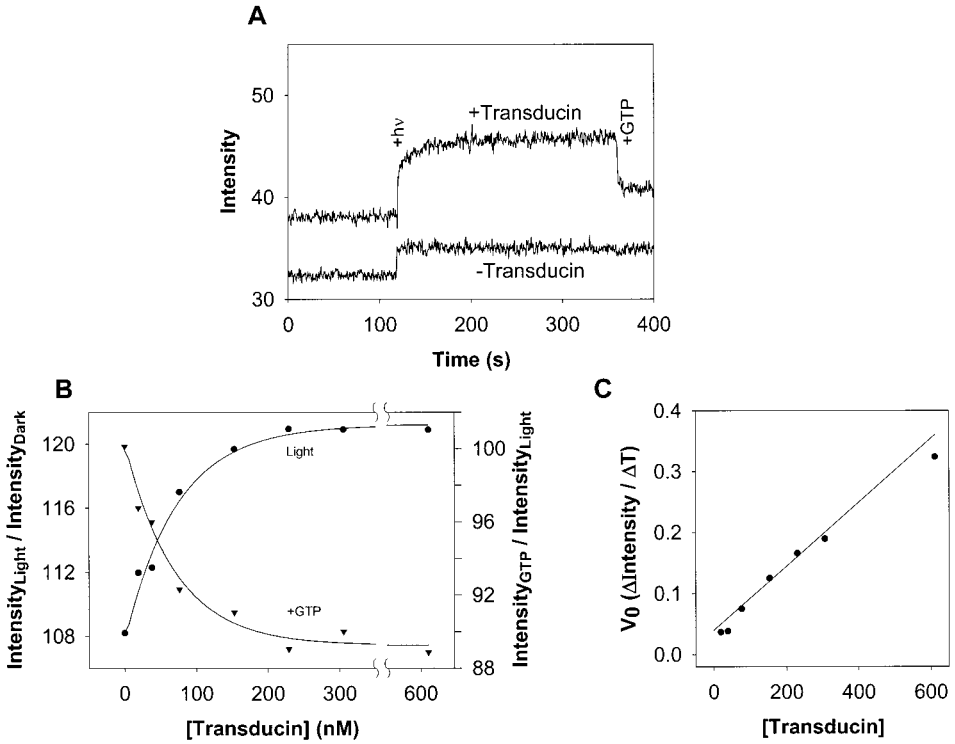

FIGURE 5: Fluorescence assay of transducin binding to the photolyzed Alexa594−rhodopsin conjugate. (A) Typical assessment of transducin binding to the photolyzed Alexa594−rhodopsin conjugate. The Alexa594−rhodopsin conjugate (35 nM) and transducin (610 nM) were suspended in HEPES buffer [50 mM HEPES, 140 mM NaCl, and 2 mM $MgCl_2$ (pH 7.5)] at 10 °C. The sample was excited by flash 120 s after recording had begun. GTP was added to the sample at 360 s (final concentration of 20 μM). (B) Fluorescence changes before and after flash (●) and before and after addition of GTP (▼) were plotted against the concentration of transducin. The concentration of the Alexa594−rhodopsin conjugate was 35 nM. (C) The rate of extra-metarhodopsin II formation, measured from the initial slope of the slow increase in fluorescence after flash excitation, was plotted as a function of transducin concentration.

Finally, a rapid decrease of the fluorescence was observed upon addition of GTP. Because the first increase is also observed without transducin, we assumed that during this phase an equilibrium between metarhodopsin I and metarhodopsin II is established. Next transducin binds to rhodopsin, stabilizes metarhodopsin II (extra-metarhodopsin II) leading to further increase, and finally dissociates upon addition of GTP. To elucidate the effect of transducin on the fluorescence property of the Alexa594−rhodopsin complex, the fluorescence assay was carried out under conditions that favored metarhodopsin II (pH 6.5 and 25 °C).The fluorescence increase just after flash without transducin (∼20%) was larger than that with transducin (∼17%), suggesting that transducin has a minor quenching effect on the fluorescence of Alexa594 immoblized on the cytoplasmic surface of rhodopsin.

The fluorescence changes induced by light or GTP as a function of transducin concentration are shown in Figure 5B. The former is the ratio between the dark fluorescence intensity and the plateau after flash, and the latter is the ratio between the plateau after flash and after addition of GTP. As the concentration of transducin increased, the change is enhanced. Therefore, the magnitude of the fluorescence change is dependent on the concentration of transducin. The first rate of extra-metarhodopsin II formation was measured from the initial slope of the slow fluorescence increase. As shown in Figure 5C, it was proportional to the concentration of transducin. The agreements of these correlations indicate that the assay using the Alexa594−rhodopsin complex is quantitative.

Competition of Unmodified Rhodopsin with the Alexa594−Rhodopsin Complex in the Transducin Assay. Chemical modification can have an effect on the function and interaction of the protein of interest with its partner protein. Therefore, it was important to determine if modification of rhodopsin by Alexa594 affected the accessibility and affinity for transducin. The effect of Alexa594 on the affinity of metarhodopsin II was tested by a competition between intact rhodopsin and modified rhodopsin for binding of transducin (Figure 6). The affinity of modified and unmodified rhodopsin for transducin appeared to be comparable in two sets of experiments. In the sample containing only the Alexa594−rhodopsin complex, a decease in rhodopsin concentration caused the ratio of fluorescence increase to be enhanced due to saturation of metarhodopsin II and maximal formation of extra-metarhodopsin II (○). In another experiment, fluorescence changes remained nearly constant while the ratio of the Alexa594−rhodopsin complex and intact rhodopsin varied from 70:0 to 5:65 (●). The fluorescence increase on flash (panel A), and decrease on addition of GTP (panel B), was observed in both experimental sets. If the affinity of unmodified rhodopsin is higher than that of modified rhodopsin, the major fraction of transducin should bind to unmodified rhodopsin, resulting in a decrease in the fluorescence change as the amount of unmodified rhodopsin is increased. Such predicted results were not observed in our experiments.

Interaction between the Photolyzed, Phosphorylated Alexa594−Rhodopsin Complex and Arrestin. Binding of arrestin to photolyzed phosphorylated rhodopsin was studied

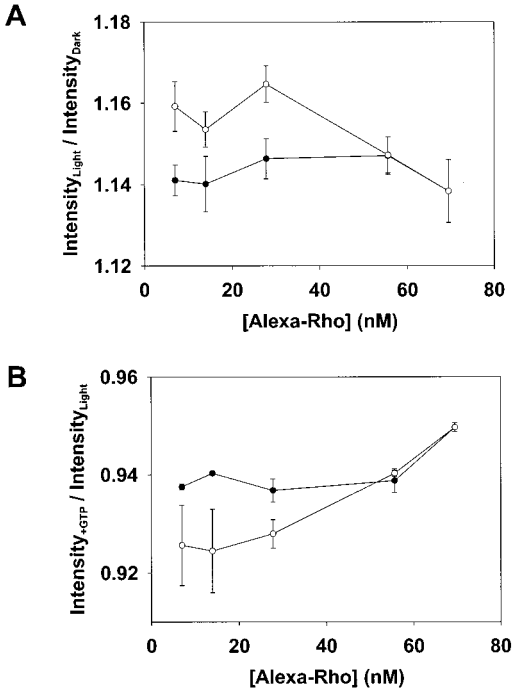

FIGURE 6: Competition of unmodified rhodopsin with the Alexa594−rhodopsin conjugate. Various concentrations of the Alexa594−rhodopsin conjugate and 70 nM transducin were suspended in HEPES buffer [50 mM HEPES, 140 mM NaCl, and 2 mM $MgCl_2$ (pH 7.5)] at 10 °C. The fluorescence changes before and after the flash (A) and before and after the addition of GTP (B) were plotted against the concentration of the Alexa594−rhodopsin conjugate (○). In complementary experiments (●), the total concentration of unmodified rhodopsin and the Alexa594−rhodopsin conjugate was constant (70 nM). Note that the concentration of the Alexa594−rhodopsin conjugate is indicated on the *x*-axis, while the concentration of unmodified rhodopsin is the difference between the total concentration of rhodopsins (70 nM) minus that of the Alexa594−rhodopsin conjugate. The fluorescence changes before and after the flash (A) and before and after the addition of GTP (B) were plotted against the concentration of the Alexa594−rhodopsin conjugate.

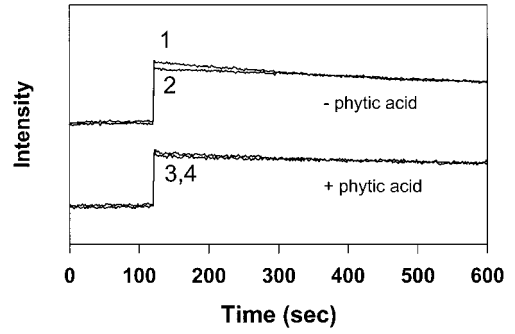

FIGURE 7: Binding of arrestin to the phosphorylated, photolyzed Alexa594−rhodopsin conjugate. Phosphorylated (traces 2 and 4) and nonphosphorylated rhodopsin in ROS membranes (traces 1 and 3) modified with Alexa594 (100 nM each) were suspended in 20 mM MES, 100 mM NaCl, and 2 mM $MgCl_2$ (pH 6.5) containing 830 nM arrestin at 25 °C. The samples for traces 3 and 4 were supplemented with phytic acid (5 mM). The sample was excited by a flash at 120 s that bleached 60% of the rhodopsin. Similar results were obtained in three independent experiments.

using the same fluorescence method (Figure 7). Rhodopsin was phosphorylated in a light-dependent manner by ATP in a reaction catalyzed by rhodopsin kinase endogenous to ROS (*14*). The product of this reaction, phosphorylated opsin, was regenerated with 11-*cis*-retinal. As a control, rhodopsin in native ROS was irradiated without ATP and regenerated. Both samples were modified by Alexa594 under the same conditions as sample 2 in Materials and Methods (1:1 stoichiometry). To establish the effect of arrestin on the fluorescence of the Alexa594−phosphorylated rhodopsin complex, the assay was carried out under conditions that favored the formation of metharhodopsin II.

Phosphorylated and nonphosphorylated rhodopsin in ROS membranes were suspended in MES buffer, and mixed with arrestin. Upon flash, the fluorescence increase in the level of nonphosphorylated rhodopsin was slightly higher than that of phosphorylated rhodopsin in native ROS membranes. In addition, the decay of phosphorylated, photolyzed rhodopsin was slower than that of nonphosphorylated, photolyzed rhodopsin. These differences are attributed to the binding of arrestin because they were not observed in the presence of phytic acid, an inhibitor of the phosphorylated, photolyzed rhodopsin−arrestin interaction (*47*, *48*). Therefore, our assay is applicable to the arrestin−metarhodopsin II interaction as well. A similar assay at pH 7.5, which favored the formation of metarhodopsin I, produced an even smaller decrease in fluorescence (data not shown). These results suggest that the conformation of the Alexa594−rhodopsin complex in the complex with arrestin differs from that of transducin.

DISCUSSION

In the work presented here, a novel method for detecting conformational changes of a protein using fluorescence probes was developed and applied to the rhodopsin system. We tested the chemical accessibility of the Alexa594−maleimide, Cy5−iodoacetoamide, and Texas Red−maleimide complexes to modify cysteine residues of rhodopsin in native membranes. The amount of Texas Red bound to the membrane was much larger than the amount of fluorophore covalently bound to the cysteine residues of rhodopsin, and Cy5 was washed out almost completely from ROS without modifying rhodopsin. In contrast, Alexa594 stoichiometrically modified rhodopsin.

When the molar ratio of rhodopsin and Alexa594 in the reaction mixture was 1:2.3, Alexa594 modified rhodopsin with a 1:0.9 stoichiometry. The thermolysin digestion followed by SDS−PAGE analysis indicated that Cys^{316} is specifically modified. This opens the possibility that the Alexa594−rhodopsin complex in native membranes could be used to monitor the local conformational changes upon illumination. Cys^{140} was modified only in the presence of a large excess of Alexa594. This result is in contrast to the fact that the accessibilities of Cys^{140} and Cys^{316} are comparable for low-molecular weight compounds, such as spin-labels (*13*, *49*). Alexa594 is a bulky fluorophore, and the hindrance around Cys^{140} may not allow efficient modification. Alternatively, Cys^{140} might be too close to the phospholipid membranes (*5*), resulting in repelling of Alexa594, which contains one carboxyl group and two sulfo groups. The advantage of selective modification is that intact ROS from the retina can be used which also contain the native lipid system and other intact structural proteins such as peripherin/ROM and the ATP-binding cassette transporter (ABCR). Since Cys^{316} is a widely conserved residue, this method is applicable to other visual pigments, and is particularly relevant to the cone pigments. Such comparative studies would be of special interest, because the kinetic

properties of the metarhodopsin II intermediates of cone pigments are known to be different from metarhodopsin II (*50*−*52*).

To detect the binding interaction of proteins, sedimentation analysis using ultracentrifugation is widely used. It is a simple method, but it is applicable mostly for the steady-state system. For example, it cannot measure the rates of rapid reactions, such as the transformations during visual transduction. Furthermore, surface plasmon resonance analysis has become recently popular (*53*, *54*). However, it frequently employs soluble proteins, or requires detergent-solubilized membrane proteins with and without added phospholipids, creating conditions that are significantly different from those found, for example, in ROS (but, see also ref *55*). Our method of using a fluorescence probe is sufficiently fast for real-time analysis, and moreover very sensitive, although the premodification by a fluorophore is essential. Fortunately, modification of rhodopsin's cysteine residues does not alter the formation of equilibrium between metarhodopsin I and metarhodpsin II, and the affinity of metarhodopsin II for transducin (*13*, *49*, *56*). Thus, modifications of the cytoplasmic surface of rhodopsin do not perturb the structure significantly.

The fluorescence intensity was enhanced as a result of the equilibrium formation between metarhodopsin I and metarhodopsin II. The fluorescence increase was larger under acidic conditions, and at 4 °C, the apparent pK_a was 6.8, which is in good agreement with previous reports (*43*, *44*, *46*). These results are consistent with large structural changes around Cys^{316} during metarhodopsin II formation. This agrees with the accepted idea that the structure of the cytoplasmic surface around this region is altered on formation of metarhodpsin II and binding of transducin (*33*−*36*, *56*), even though this region most likely is not essential for the binding and activation of transducin. This is because truncated rhodopsin, lacking the Cys^{316} region and C-terminus, is still active (*57*, *58*).

In the presence of transducin, an increase in fluorescence was observed, and was attributed to the increased population of metarhodopsin II, so-called extra-metarhodopsin II (*20*, *22*). Upon addition of GTP, the fluorescence rapidly decreased to the level observed in the absence of transducin. Therefore, the formation of extra-metarhodopsin II is clearly and reproducibly observed in this system. In the presence of arrestin, the behavior of phosphorylated metarhodopsin II and unphosphorylated metarhodopsin II differed; however, this difference was lost in the presence of phytic acid, an inhibitor of arrestin binding to phosphorylated photolyzed rhodopsin (*47*, *48*). These results suggest that this effect was a result of arrestin binding. It should be noted that the increase in fluorescence for the phosphorylated metarhodopsin II was smaller than for unphosphorylated metarhodopsin II.

UV−visible spectroscopy has shown that the absorbance increase at 380 nm after photoexcitation of phosphorylated rhodopsin in the presence of arrestin is larger than in the absence of arrestin (*24*, *59*). Thus, extra-metarhodposin II is thought to be formed by binding of arrestin to metarhodopsin II, like transducin binds to metarhodopsin II. In contrast, the results presented here show that the fluorescence increase for phosphorylated rhodopsin in the presence of arrestin was slightly smaller than in the absence of arrestin. Therefore, the cytoplasmic surface structure of extra-metarhodopsin II with arrestin is different from metarhodopsin II and extra-metarhodopsin II with transducin, which increases the level of fluorescence. The absorbance increase at 380 nm indicates the deprotonation of the retinal Schiff base chromophore. Therefore, deprotonation does not necessarily induce the same structural change of the cytoplasmic surface of the phosphorylated metarhodopsin II−Alexa594 complex in the complex with arrestin. Arrestin not only would block the binding site of transducin but also could alter the structure of the cytoplasmic surface to terminate the light signal transduction cascade. Specific interactions of arrestin with immobilized Alexa594 lead to quenching of fluorescence rather than its enhancement. Apart from the interpretation, this assay could be very useful in studying transducin− or arrestin−metarhodopsin II (intermediates of cone pigments) interactions and should be optimized for low levels of bleaches.

In summary, a novel continuous fluorescence assay has been developed for detecting the light-induced conformational changes of rhodopsin. Significant conformation changes were detected in rhodopsin at Cys^{316} region upon illumination. This is particularly interesting, as this region of rhodopsin forms an extra α-helix that runs parallel to the surface of membranes (*5*). The function of this region has not been fully defined yet. An additional advantage of this assay is the ability to use rhodopsin in native membranes. Changes in fluorescence were also exploited to monitor the interaction between photolyzed rhodopsin and G-protein or arrestin.

ACKNOWLEDGMENT

We thank J. Preston Van Hooser for technical help during the course of this study, Dr. Carola A. G. G. Driessen, Dr. Tom Ebrey, Dr. Klaus Peter Hofmann, Dr. Tetsuji Okada, and Joshua K. McBee for comments on the manuscript, Dr. Robert N. Fariss for suggestions on use of Alexa compounds for rhodopsin modification, and Dr. Tetsuji Okada for help with the preparation of Figure 1.

REFERENCES

1. Yoshizawa, T., and Wald, G. (1963) *Nature 197*, 1279−1286.
2. Wald, G. (1968) *Science 162*, 230−239.
3. Bownds, D. (1967) *Nature 216*, 1178−1181.
4. Hargrave, P. A., McDowell, J. H., Curtis, D. R., Wang, J. K., Juszczak, E., Fong, S. L., Rao, J. K., and Argos, P. (1983) *Biophys. Struct. Mech. 9*, 235−244.
5. Palczewski, K., Kumasaka, T., Hori, T., Behnke, C. A., Motoshima, H., Fox, B. A., Le Trong, I., Teller, D. C., Okada, T., Stenkamp, R. E., Yamamoto, M., and Miyano, M. (2000) *Science 289*, 739−745.
6. Shichida, Y., and Imai, H. (1998) *Cell Mol. Life Sci. 54*, 1299−1315.
7. Sakmar, T. P., Franke, R. R., and Khorana, H. G. (1989) *Proc. Natl. Acad. Sci. U.S.A. 86*, 8309−8313.
8. Zhukovsky, E. A., and Oprian, D. D. (1989) *Science 246*, 928−930.
9. Fahmy, K., Jager, F., Beck, M., Zvyaga, T. A., Sakmar, T. P., and Siebert, F. (1993) *Proc. Natl. Acad. Sci. U.S.A. 90*, 10206−10210.
10. Arnis, S., and Hofmann, K. P. (1993) *Proc. Natl. Acad. Sci. U.S.A. 90*, 7849−7853.
11. Meyer, C. K., Bohme, M., Ockenfels, A., Gartner, W., Hofmann, K. P., and Ernst, O. P. (2000) *J. Biol. Chem. 275*, 19713−19718.

12. Doukas, A. G., Aton, B., Callender, R. H., and Ebrey, T. G. (1978) *Biochemistry 17*, 2430−2435.
13. Resek, J. F., Farahbakhsh, Z. T., Hubbell, W. L., and Khorana, H. G. (1993) *Biochemistry 32*, 12025−12032.
14. Kühn, H. (1978) *Biochemistry 17*, 4389−4395.
15. Kühn, H. (1980) *Nature 283*, 587−589.
16. Kühn, H., Hall, S. W., and Wilden, U. (1984) *FEBS Lett. 176*, 473−478.
17. Wilden, U., and Kühn, H. (1982) *Biochemistry 21*, 3014−3022.
18. Farahbakhsh, Z. T., Ridge, K. D., Khorana, H. G., and Hubbell, W. L. (1995) *Biochemistry 34*, 8812−8819.
19. Kim, J.-M., Altenbach, C., Thurmond, R. L., Khorana, H. G., and Hubbell, W. L. (1997) *Proc. Natl. Acad. Sci. U.S.A. 94*, 14273−14278.
20. Hofmann, K. P., Emeis, D., and Schnetkamp, P. P. (1983) *Biochim. Biophys. Acta 725*, 60−70.
21. Emeis, D., Kühn, H., Reichert, J., and Hofmann, K. P. (1982) *FEBS Lett. 143*, 29−34.
22. Emeis, D., and Hofmann, K. P. (1981) *FEBS Lett. 136*, 201−207.
23. Bennett, N., Michel-Villaz, M., and Kühn, H. (1982) *Eur. J. Biochem. 127*, 97−103.
24. Schleicher, A., Kühn, H., and Hofmann, K. P. (1989) *Biochemistry 28*, 1770−1775.
25. Konig, B., Arendt, A., McDowell, J. H., Kahlert, M., Hargrave, P. A., and Hofmann, K. P. (1989) *Proc. Natl. Acad. Sci. U.S.A. 86*, 6878−6882.
26. Raman, D., Osawa, S., and Weiss, E. R. (1999) *Biochemistry 38*, 5117−5123.
27. Palczewski, K., Buczyło, J., Kaplan, M. W., Polans, A. S., and Crabb, J. W. (1991) *J. Biol. Chem. 266*, 12949−12955.
28. Titus, J. A., Haugland, R., Sharrow, S. O., and Segal, D. M. (1982) *J. Immunol. Methods 50*, 193−204.
29. Mujumdar, R. B., Ernst, L. A., Mujumdar, S. R., Lewis, C. J., and Waggoner, A. S. (1993) *Bioconjugate Chem. 4*, 105−111.
30. Panchuk-Voloshina, N., Haugland, R. P., Bishop-Stewart, J., Bhalgat, M. K., Millard, P. J., Mao, F., Leung, W. Y., and Haugland, R. P. (1999) *J. Histochem. Cytochem. 47*, 1179−1188.
31. Ovchinnikov, Yu. A. (1982) *FEBS Lett. 148*, 179−191.
32. Ovchinnikov, Yu. A., Abdulaev, N. G., and Bogachuk, A. S. (1988) *FEBS Lett. 230*, 1−5.
33. Yang, K., Farrens, D. L., Altenbach, C., Farahbakhsh, Z. T., Hubbell, W. L., and Khorana, H. G. (1996) *Biochemistry 35*, 14040−14046.
34. Cai, K., Klein-Seetharaman, J., Hwa, J., Hubbell, W. L., and Khorana, H. G. (1999) *Biochemistry 38*, 12893−12898.
35. Yu, H. B., Kono, M., and Oprian, D. D. (1999) *Biochemistry 38*, 12028−12032.
36. Gelasco, A., Crouch, R. K., and Knapp, D. R. (2000) *Biochemistry 39*, 4907−4914.
37. Fukada, Y., Okano, T., Shichida, Y., Yoshizawa, T., Trehan, A., Mead, D., Denny, M., Asato, A. E., and Liu, R. S. H. (1990) *Biochemistry 29*, 3133−3140.
38. Wald, G., and Brown, P. K. (1952) *J. Gen. Physiol. 35*, 797−816.
39. Buczyło, J., and Palczewski, K. (1993) *Methods Neurosci. 15*, 226−236.
40. Hargrave, P. A. (1982) in *Progress in Retinal Research* (Osbourne, N. N., and Chader, G. J., Eds.) pp 1−51, Pergamon Press, New York.
41. Findlay, J. B. C., Barclay, P. L., Brett, M., Davison, M., Pappin, D. J. C., and Thompson, P. (1984) *Vision Res. 24*, 1501−1508.
42. Papac, D. I., Thornburg, K. R., Bullesbach, E. E., Crouch, R. K., and Knapp, D. R. (1992) *J. Biol. Chem. 267*, 16889−16894.
43. Matthews, R. G., Hubbard, R., Brown, P. K., and Wald, G. (1963) *J. Gen. Physiol. 47*, 215−240.
44. Bennett, N. (1978) *Biochem. Biophys. Res. Commun. 83*, 457−465.
45. Imai, H., Mizukami, T., Imamoto, Y., and Shichida, Y. (1994) *Biochemistry 33*, 14351−14358.
46. Parkes, J. H., Gibson, S. K., and Liebman, P. A. (1999) *Biochemistry 38*, 8598−8598.
47. Palczewski, K., Pulvermûller, A., Buczyło, J., Gutmann, C., and Hofmann, K. P. (1991) *FEBS Lett. 295*, 195−199.
48. Palczewski, K., Rispoli, G., and Detwiler, P. B. (1992) *Neuron 8*, 117−126.
49. Resek, J. F., Farrens, D., and Khorana, H. G. (1994) *Proc. Natl. Acad. Sci. U.S.A. 91*, 7643−7647.
50. Okada, T., Matsuda, T., Kandori, H., Fukada, Y., Yoshizawa, T., and Shichida, Y. (1994) *Biochemistry 33*, 4940−4946.
51. Imai, H., Imamoto, Y., Yoshizawa, T., and Shichida, Y. (1995) *Biochemistry 34*, 10525−10531.
52. Imai, H., Terakita, A., Tachibanaki, S., Imamoto, Y., Yoshizawa, T., and Shichida, Y. (1997) *Biochemistry 36*, 12773−12779.
53. Ernst, O. P., Bieri, C., Vogel, H., and Hofmann, K. P. (2000) *Methods Enzymol. 315*, 471−489.
54. Salamon, Z., Brown, M. F., and Tollin, G. (1999) *Trends Biochem. Sci. 24*, 213−219.
55. Bieri, C., Ernst, O. P., Heyse, S., Hofmann, K. P., and Vogel, H. (1999) *Nat. Biotechnol. 17*, 1105−1108.
56. Ernst, O. P., Meyer, C. K., Marin, E. P., Henklein, P., Fu, W. Y., Sakmar, T. P., and Hofmann, K. P. (2000) *J. Biol. Chem. 275*, 1937−1943.
57. Osawa, S., and Weiss, E. R. (1994) *Mol. Pharmacol. 46*, 1036−1040.
58. Weiss, E. R., Osawa, S., Shi, W., and Dickerson, C. D. (1994) *Biochemistry 33*, 7587−7593.
59. Gibson, S. K., Parkes, J. H., and Liebman, P. A. (2000) *Biochemistry 39*, 5738−5749.

BI0018685